Prediction of Membrane Permeability to Peptides from Calculated Dynamic Molecular Surface Properties

Patric Stenberg,[1] Kristina Luthman,[2] and Per Artursson[1,3]

Received July 28, 1998; accepted November 11, 1998

Purpose. To develop a theoretical method for prediction of transcellular permeability to peptides.

Methods. The dynamic molecular surface properties of 19 oligopeptide derivatives, divided into three homologous series were calculated. The dynamic molecular surface properties were compared with commonly used experimental predictors of membrane permeability such as partition coefficients. Relationships between the dynamic molecular surface properties and intestinal epithelial permeability, as determined in Caco-2 cell monolayers, were used to develop a model for prediction of the transmembrane permeability to the oligopeptide derivatives.

Results. A theoretical model was derived which takes both the polar and non-polar part of the dynamic molecular surface area of the investigated molecule into consideration. The model provided a strong relationship with transepithelial permeability for the oligopeptide derivatives. The predictability of transepithelial permeability from this model was comparable to that from the best experimental descriptor.

Conclusions. To our knowledge, this is the first example of a theoretical model that gives a satisfactory relationship between calculated molecular properties and epithelial permeability to peptides by accounting for both the hydrogen bonding capacity and the hydrophobicity of the investigated molecule. This model may be used to differentiate poorly absorbed oligopeptide drugs at an early stage of the drug discovery process.

KEY WORDS: molecular surface area; hydrogen bonding; lipophilicity; intestinal drug transport; Caco-2 cells.

INTRODUCTION

The poor biopharmaceutical characteristics of pharmacologically active peptides and peptide derivatives constitute a major reason for their low success rates in clinical development (1). Apart from their metabolic instability, peptides generally also display severely limited transport across tissue barriers such as the intestinal epithelium (2,3). The reasons for this limited transport remain poorly understood. The development of methodologies that can increase our understanding of the molecular properties influencing transcellular transport and also predict epithelial permeability to peptide derivatives is therefore of profound importance.

Experimentally and theoretically determined molecular properties such as lipophilicity, hydrogen bonding potential and molecular size are commonly used as rough predictors of membrane permeability to peptides as well as conventional drugs (2,4). The correlations between these descriptors and membrane permeability are of an acceptable standard only for series of homologous compounds and are frequently impaired when structural diversity is introduced (5–8). In general, molecular properties related to hydrogen bonding capacity have provided the best correlations with the membrane permeability to peptide derivatives (9,10). Some complex combinations of molecular descriptors have been used to improve these correlations but there is no real consensus with regard to the method of choice (7).

The explosive development of computer technology has generated new methods for the calculation of molecular descriptors. Such theoretically derived descriptors are particularly attractive in predictions of membrane permeability since they may be used to differentiate poorly absorbed peptides at an early stage of the drug discovery process (4). The contribution of various calculated molecular descriptors to the permeability of intestinal epithelial cell membranes to drug molecules has recently been investigated using multivariate analysis (e.g., 11,12). While these methods may generate acceptable correlations with membrane permeability, they do not generally consider the three-dimensional shape and the conformational flexibility of the molecule.

Recently, we developed a theoretical method for the prediction of drug absorption, based on the determination of the dynamic surface properties of drug molecules (13,14). This method has the advantage of accounting for the shape and flexibility of the drug molecule (13). The dynamic polar surface area (PSA_d), which is related to the molecular hydrogen bonding capacity, was found to provide an excellent relationship with intestinal epithelial permeability to a homologous series of drugs in vitro (13) and surprisingly also with the proportion of an oral dose absorbed after administration of structurally diverse drugs to humans (14). However, these results were obtained using conventional drugs with limited flexibility. It therefore remains to be established whether molecular surface properties such as the dynamic polar surface area are also applicable as predictors of membrane permeability to more flexible molecules such as peptides and peptide derivatives.

In this study, we examine the dynamic molecular surface properties of 19 oligopeptide derivatives, divided into three homologous series. The dynamic molecular surface properties were compared with commonly used experimental predictors of membrane permeability such as octanol-water, heptane-ethylene glycol and heptane-octanol partitioning (9,15). Relationships between the dynamic molecular surface properties and intestinal epithelial permeability, as determined in Caco-2 cell monolayers (15), were used to develop a model for prediction of intestinal permeability to the oligopeptide derivatives. Two series of dipeptide derivatives, each containing six compounds with the same number of hydrogen bonding groups and hydrogen bonding moieties (AcHN-X-phenethylamide and AcHN-X-D-Phe-NHMe, respectively), were used for model development. A structurally different third series of D-Phe oligomers was used to test the derived model.

METHODS

Oligopeptides

Nineteen oligopeptide derivatives were investigated (Fig. 1). Epithelial permeability data and partition coefficients of the

[1] Department of Pharmaceutics, Uppsala Biomedical Centre, Uppsala University, P.O. Box 580, SE-751 23 Uppsala, Sweden.

[2] Department of Medicinal Chemistry, Institute of Pharmacy, University of Tromsø, N-9037 Tromsø, Norway.

[3] To whom correspondence should be addressed. (e-mail: per.artursson@galenik.uu.se)

0724-8741/99/0200-0205$16.00/0

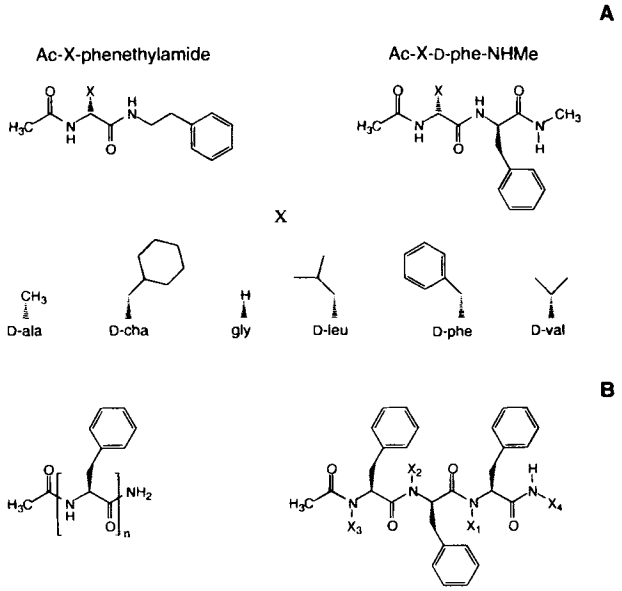

Peptide	n	X_1	X_2	X_3	X_4
Ac-D-phe-NH_2	1				
Ac-D-phe_2-NH_2	2				
Ac-D-phe_3-NH_2	3				
Ac-D-phe_2-(NMe-D-phe)-NH_2		CH_3	H	H	H
Ac-D-phe-(NMe-D-$phe)_2$-NH_2		CH_3	CH_3	H	H
Ac-$(NMe\text{-}D\text{-}phe)_3$-$NH_2$		CH_3	CH_3	CH_3	H
Ac-$(NMe\text{-}D\text{-}phe)_3$-NHMe		CH_3	CH_3	CH_3	CH_3

Fig. 1. Structures of peptide derivatives investigated in this study. The AcHN-X-phenethylamide and AcHN-X-D-Phe-NHMe dipeptide derivatives (A) were used to develop the model. The structurally different D-Phe-oligomers (B) were used to test the model.

AcHN-X-phenethylamide and AcHN-X-D-Phe-NHMe derivatives were obtained from Dr. Jay Goodwin, Pharmacia & Upjohn Inc., Kalamazoo (15) and data on the D-Phe oligomers were obtained from (9) and (15).

Cell Culture and Transport Experiments

Caco-2 cell monolayer permeabilities for the 19 peptide derivatives were determined by others (15). Since the experimental methodology is slightly different from previous publications (9), a brief description of the methodology is given: Caco-2 cells were cultured on Transwell polycarbonate filters (24 mm diameter; pore size 0.4 μm; Costar). Both the apical and the basolateral solutions contained 300 μM verapamil to inhibit P-glycoprotein-mediated efflux (16). Effective Caco-2 cell monolayer permeabilities were calculated using the following equation:

$$Papp = \frac{dC}{dt} \cdot \frac{V}{A \cdot C_0} \quad (1)$$

where dC/dt is the increase in concentration in the receiver compartment over time, V the volume of the receiver compartment, A the filter area and C_0 the peptide concentration in the donor solution.

Partition Coefficients

Octanol-water ($logP_{o/w}$), heptane-water ($logP_{h/w}$), isooctane-water and heptane-ethylene glycol ($logP_{h/eg}$) partition coefficients were obtained from the literature (9,15). ΔlogP for the AcHN-X-phenethylamide and AcHN-X-D-Phe-NHMe dipeptide derivatives was obtained from the difference between the logarithms of the octanol-water and the heptane-water partition coefficients. ΔlogP for the D-Phe oligomers was determined from the difference between the logarithms of the octanol-water and the isooctane-water partition coefficients. It has been shown (17) that solute partitioning in the heptane-water and the octane-water systems is sufficiently similar to be directly comparable.

Maximum Number of Hydrogen Bonds

The maximum number of hydrogen bonds that each compound can form (Ht) was calculated by assuming that every hydrogen atom that can participate in hydrogen bonding will contribute +1 to the number of hydrogen bond donors (Hd). Similarly, the method assumes contributions to hydrogen bond acceptors (Ha) of +1 for nitrogen atoms and +2 for oxygen atoms. Ht is the sum of Ha and Hd (14).

Conformational Analysis

The conformational analysis was initiated with a 1000-step Monte Carlo conformational search (18) using the AMBER force field in MacroModel v5.0 (19) on Silicon Graphics Indy and O2 workstations. The global minima from these calculations were then used as starting points for subsequent 5000- (Ac-D-phe-NH_2) or 10,000-step (all others) Monte Carlo searches. By using this procedure, it was assumed that the entire conformational space of low energy conformations ($\Delta E_S \leq 2.5$ kcal/mol) would be covered. The low energy conformations obtained from the two searches were then pooled and duplicates were removed. An additional conformational analysis was undertaken by a 3000- to 20,000-step Monte Carlo search in a simulated water environment using the global minima from the analyses without solvent as starting geometries.

Surface Area Calculations

An in-house computer program (MAREA)[4] was used to calculate the surface area of each conformer as described previously (14). The program calculates the free surface area of each atom as well as the molecular volume (V). The atomic van der Waals radii used were the following: sp^2 carbons 1.94 Å, sp^3 carbon 1.90 Å, oxygen 1.74 Å, nitrogen 1.82 Å, electroneutral hydrogen 1.50 Å, hydrogen bonded to oxygen 1.10 Å and hydrogen bonded to nitrogen 1.125 Å (obtained from PCMODEL v4.0 see 20).

The polar surface area (PSA) was defined as the area occupied by nitrogen and oxygen atoms, plus the area of the hydrogen atoms attached to these heteroatoms. The non-polar part of the surface area (NPSA) was defined as the total surface area (SA) minus PSA. We also calculated the percentage of the surface area occupied by polar groups (%PSA).

[4] The program MAREA is available upon request from the authors. The program is provided free of charge for academic users. The surface areas calculated by this program differ slightly from those obtained from calculations in PCMODEL v4.0 reported elsewhere (13). This is due to: i. PCMODEL uses a grid-based numerical algorithm for surface area calculations, and ii. the definition of polar surface area in PCMODEL also includes carbonyl carbon atoms.

The dynamic surface area (SA_d) is a statistical average obtained by weighting the surface area of each low energy conformation ($\Delta E_s \leq 2.5$ kcal/mol) by its probability of existence according to a Boltzmann distribution (13,21). The dynamic polar surface area (PSA_d), dynamic non-polar surface area ($NPSA_d$), percentage of the total dynamic surface area that is polar (%PSA_d) and dynamic volume (V_d) were determined in the same manner.

Data Analysis

Multiple sigmoidal and linear regression was performed using Microsoft EXCEL5.0 for Macintosh. A linear combination of PSA_d and $NPSA_d$ ($k_1 \times PSA_d - k_2 \times NPSA_d$) was used to describe Caco-2 cell monolayer permeability by the sigmoidal relationship

$$P_{app} = \frac{P_{app,max}}{1 + \left(\frac{k_1 \cdot PSA_d + k_2 \cdot NPSA_d}{Surface_{50\%}}\right)^{\gamma}} \quad (2)$$

where k_1 and k_2 are the weights assigned to the dynamic polar and dynamic non-polar surface areas, respectively. $P_{app,max}$ is the plateau value of the function, $Surface_{50\%}$ is the value of $k_1 \times PSA_d - k_2 \times NPSA_d$ at half $P_{app,max}$ and γ is a slope factor.

The equation was fitted to the permeability data by minimizing the sum of squared residuals. The coefficient k_1 was kept constant at 1 since it is the relationship rather than the absolute numbers of k_1 and k_2 that is important. In order to assure that the global minima were found, the iterative procedure was repeated with different starting points. The sigmoidal model was chosen since it has been shown that the permeability levels out at high and low transport rates. The higher plateau is reached as factors other than membrane transport (i.e., the unstirred water layer) become rate limiting for the permeation process (22). The lower plateau of the sigmoidal curve is associated with paracellular transport of the molecule through the epithelial cell monolayer. The fit of the model was calculated as R^2, the coefficient of determination, which is the sum of squared residuals from the regression divided by the total sum of squared residuals in the data set. The predictability of the model was assessed by the leave-one-out cross-validated R^2. The strength of linear relationships was assessed by the correlation coefficient, r.

RESULTS

Peptide Derivatives

The dependence of intestinal epithelial Caco-2 cell permeability (P_{app}) on the molecular surface properties was studied using the 19 oligopeptide derivatives detailed in Table I (15). Twelve of these were distributed into two homologous series, each containing six dipeptide derivatives (derivatives of AcHN-X-phenethylamide and AcHN-X-D-Phe-NHMe, respectively; Fig. 1A). The dipeptide derivatives within each of these series were designed to have the same number of potential hydrogen bonds. In addition, all twelve dipeptide derivatives contained the same type of hydrogen bonding moieties. These twelve peptide derivatives were used for development of a theoretical model for prediction of membrane permeability.

A third set of seven D-Phe oligomers (Fig. 1B) was used to assess the applicability of the derived model to a structurally different set of peptides (9). This set differed from those used

Table I. Epithelial Permeability, Structural, and Physico-Chemical Properties of the Oligopeptide Derivatives Investigated in this Study

Compound[a]	log P_{app}[b] (cm/s)	$NPSA_d$[c] vacuum (Å^2)	PSA_d[c] vacuum (Å^2)	V_d[c] vacuum (Å^3)	$NPSA_d$[c] water (Å^2)	PSA_d[c] water (Å^2)	V_d[c] water (Å^3)	Ha[c]	Hd[c]	Ht[c]	$logP_{o/w}$[b]	$\Delta logP$[d]	$logP_{h/eg}$[d]
AcHN-D-ala-D-phe-NHMe	−4.60	257.4	53.9	300.9	266.5	58.8	303.9	6	2	8	0.76	4.29	−4.40
AcHN-D-cha-D-phe-NHMe	−4.26	365.4	52.0	416.4	365.1	56.3	419.0	6	2	8	3.13	4.03	−3.41
AcHN-gly-D-phe-NHMe	−4.65	233.3	57.5	277.8	245.0	61.7	280.1	6	2	8	0.48	4.21	−5.00
AcHN-D-leu-D-phe-NHMe	−4.32	321.4	52.1	367.3	320.5	56.5	368.6	6	2	8	2.03	4.17	−3.69
AcHN-D-phe_2-NHMe	−4.26	341.0	50.7	392.7	346.8	56.7	394.2	6	2	8	2.32	4.32	−3.70
AcHN-D-val-D-phe-NHMe	−4.45	300.1	50.8	344.5	304.5	54.6	346.5	6	2	8	1.59	4.23	−3.77
AcHN-D-ala-phenethylamide	−6.60	291.5	77.8	359.9	296.2	87.5	362.8	9	3	12	−0.06	6.20	−5.83
AcHN-D-cha-phenethylamide	−5.05	402.1	75.0	476.7	404.5	85.0	478.7	9	3	12	2.40	5.81	−5.03
AcHN-gly-phenethylamide	−6.85	273.2	84.6	337.2	275.3	90.9	340.4	9	3	12	−0.30	6.00	−6.17
AcHN-D-leu-phenethylamide	−5.82	358.2	75.1	426.4	359.8	85.2	429.6	9	3	12	1.24	5.85	−5.43
AcHN-D-phe-phenethylamide	−5.55	377.2	75.8	450.8	385.0	85.2	454.0	9	3	12	1.44	5.59	−5.34
AcHN-D-val-phenethylamide	−6.05	335.5	74.4	402.7	338.1	83.5	405.5	9	3	12	0.66	5.99	−5.79
Ac-D-phe-NH_2	−5.10	202.1	69.6	251.7	199.4	75.6	252.6	6	3	9	0.05	4.97	−5.46
Ac-D-phe_2-NH_2	−5.70	333.7	88.0	423.6	340.7	97.3	426.5	9	4	13	1.19	6.48	−6.52
Ac-D-phe_3-NH_2	−5.64	443.9	108.0	599.2	455.1	116.9	603.8	12	5	17	2.30	7.32	−7.10
Ac-D-phe_2-(NMe-D-phe)-NH_2	−5.17	492.9	93.2	623.2	473.2	109.4	621.6	12	4	16	2.63	6.83	−6.28
Ac-D-phe-(NMe-D-$phe)_2$-NH_2	−4.92	492.7	94.3	645.8	485.0	103.4	644.9	12	3	15	2.53	5.63	−5.14
Ac-$(NMe\text{-}D\text{-}phe)_3$-$NH_2$	−4.58	510.7	87.8	665.7	510.0	92.0	671.5	12	2	14	2.92	4.59	−4.20
Ac-$(NMe\text{-}D\text{-}phe)_3$-NHMe	−4.49	552.5	74.0	692.2	554.5	78.4	694.4	12	1	13	3.24	3.93	−2.86

[a] See Fig. 1 for compound structures.
[b] Data were obtained from (15).
[c] Structural descriptors were determined as described in the Methods section.
[d] Data were obtained from (15) except for those pertaining to the D-Phe oligomers which were obtained from (9).

for model development both in molecular size and in the number of potential hydrogen bonds in each compound. The variability in hydrogen bond number was achieved by increasing the chain length and by methylation of amide nitrogen atoms. The variation in size within the series of D-Phe oligomers is greater than that in the two series used for model development (Table I). All 19 oligopeptide derivatives are uncharged at the pH (7.4) used for the permeability studies.

Use of a Simulated Water Environment in the Conformational Analyses

Conformational searches performed without solvent resulted in folded conformations (Table I) often stabilized by intramolecular hydrogen bonds. In contrast, conformational searches performed in simulated water produced elongated conformers with larger PSA which allowed stronger interactions between polar functional groups and the surrounding solvent. In spite of this, relationships between the surface properties of the compounds and P_{app}, and those between the surface properties and the physico-chemical properties of the compounds were similar irrespective of the solvent environment used in the conformational searches. The correlations between molecular surface properties calculated from conformational searches in both water and without solvent were also strong (r^2 was not less than 0.95 for any surface property). Therefore, in the following only surface properties calculated from conformational searches in simulated water are presented unless otherwise stated.

Model Development

The PSA_d values of the six AcHN-X-phenethylamide derivatives were significantly different from those of the six less permeable AcHN-X-D-Phe-NHMe derivatives. However, the ranking of the dipeptide derivatives within each series according to their P_{app} values was poorly described by PSA_d (Fig. 2A). A similar pattern was observed when ΔlogP was plotted against P_{app} (Fig. 2B). Both PSA_d and ΔlogP displayed little variability within each of the two series of dipeptide derivatives.

In contrast, the calculated $NPSA_d$ gave a rank order which correlated with P_{app} within each of the AcHN-X-phenethylamide and AcHN-X-D-Phe-NHMe derivative series. However, $NPSA_d$ failed to predict the differences in P_{app} between the series (Fig. 3A). The size descriptors SA_d and V_d as well as $\%PSA_d$ gave similar relationships to those provided by $NPSA_d$ when plotted against P_{app} (data not shown). Experimentally determined $logP_{o/w}$ gave a rank order correlation with P_{app} within the series, comparable to that obtained with $NPSA_d$ (Fig. 3B). A strong correlation was observed between $NPSA_d$ and $logP_{o/w}$ within each series of dipeptide derivatives (r^2 = 0.96 and 0.98, respectively). The corresponding correlation coefficients for conformers generated by conformational searches without solvent were 0.97 and 0.98, respectively.

Thus, none of the investigated single molecular surface properties correlated well with P_{app} for all twelve peptide derivatives used for model development. Apparently, $NPSA_d$ describes the variability in P_{app} within each series while PSA_d accounts for the variability in P_{app} between the series. A linear combination of PSA_d and $NPSA_d$ was therefore investigated. $PSA_d - 0.09 \times NPSA_d$ (k_2 = 0.09 was obtained by minimizing the sum of squared residuals in eq. 2) was found to have a strong sigmoidal relationship with P_{app} (Fig. 4A; R^2 = 0.96). The predictability of the derived model was also high; the leave-one-out cross-validated R^2 was 0.91. A similar but inverted sigmoidal relationship was obtained between $logP_{h/eg}$ and P_{app} (Fig. 4B; R^2 = 0.93). An excellent correlation was also obtained between $logP_{h/eg}$ and $PSA_d - 0.09 \times NPSA_d$ (r^2 = 0.96). $PSA_d - 0.09 \times NPSA_d$ also correlated with ΔlogP and to some extent with $logP_{o/w}$ (Table II). The combination of surface properties best describing P_{app} for conformations generated by conformational searches without solvent was $PSA_d - 0.06 \times NPSA_d$ (R^2 = 0.96).

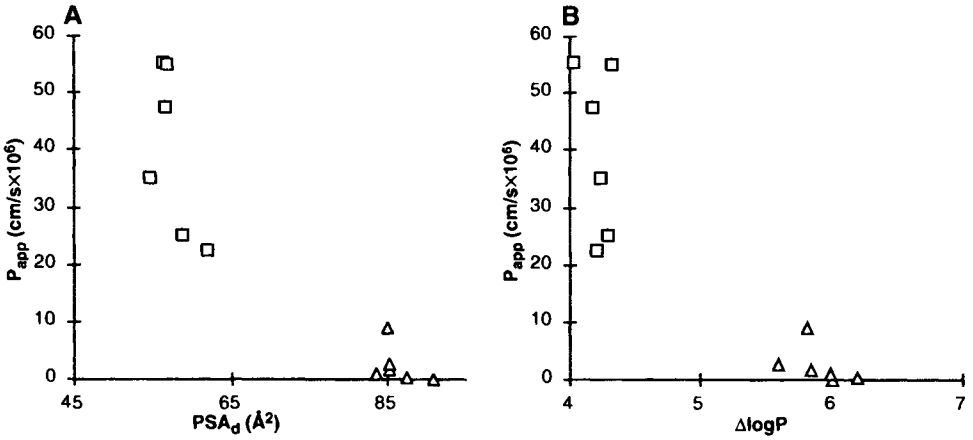

Fig. 2. Relationship between Caco-2 cell monolayer permeability (P_{app}) to and hydrogen bonding properties of two series of dipeptide derivatives. It was possible to discriminate between the two series (AcHN-X-phenethylamide (□) and AcHN-X-D-Phe-NHMe (Δ) dipeptide derivatives) using dynamic polar surface area (PSA_d), but this parameter resulted in weak relationships with permeability within each of the series (A). Similarly, it was possible to discriminate between the two series using ΔlogP, but not to rank permeability within each series (B). Calculation of PSA_d was based on conformational searches in simulated water.

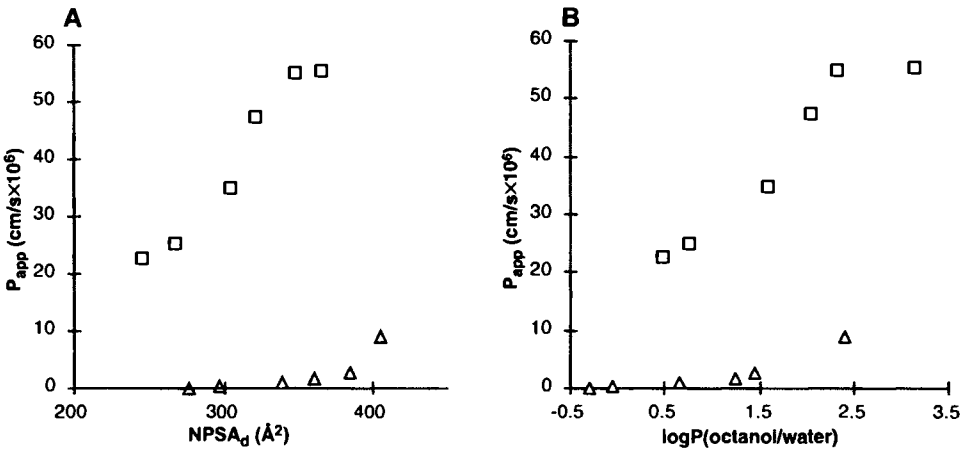

Fig. 3. Relationship between Caco-2 cell monolayer permeability (P_{app}) to and lipophilicity of two series comprising AcHN-X-phenethylamide (□) and AcHN-X-D-Phe-NHMe (Δ) dipeptide derivatives, respectively. A rank order correlation exists between dynamic non-polar surface area ($NPSA_d$) and P_{app} within each series, but $NPSA_d$ failed to account for inter-series variability in P_{app} (A). A similar pattern was observed when correlating permeability with $logP_{o/w}$, the logarithm of the octanol-water partition coefficient (B). Calculation of $NPSA_d$ was based on conformational searches in simulated water.

A series of structurally different D-Phe oligomers (Fig. 1B) was used to test the applicability of the derived expression $PSA_d - 0.09 \times NPSA_d$. In general, $PSA_d - 0.09 \times NPSA_d$ underestimated the P_{app} of most of the D-Phe oligomers, resulting in a decrease in R^2 to 0.88 (Fig. 4A). However, the combination of surface properties gave a stronger rank order correlation with P_{app} for the D-Phe oligomers than any of the surface properties alone. The experimentally determined descriptor $logP_{h/eg}$ also displayed a weaker relationship with P_{app} as the D-Phe oligomers were introduced ($R^2 = 0.81$). However, $logP_{h/eg}$ gave a slightly stronger rank order correlation with P_{app} for the D-Phe oligomers than $PSA_d - 0.09 \times NPSA_d$ (Fig. 4B). A strong correlation between $PSA_d - 0.09 \times NPSA_d$ and $logP_{h/eg}$ was obtained also after inclusion of the D-Phe oligomers ($r^2 = 0.90$). The relationship between $PSA_d - 0.06 \times NPSA_d$ and P_{app} for conformers generated by conformational searches without solvent also became slightly weaker as the D-Phe oligomers were introduced ($R^2 = 0.84$).

DISCUSSION

In this study, the relationship between experimentally and theoretically determined molecular properties and epithelial permeability was investigated. A theoretical model was derived which takes both the polar and non-polar parts of the dynamic surface area of the investigated molecule into consideration. The predictability of epithelial permeability from this model is comparable to that from the best experimental descriptor, $logP_{h/eg}$.

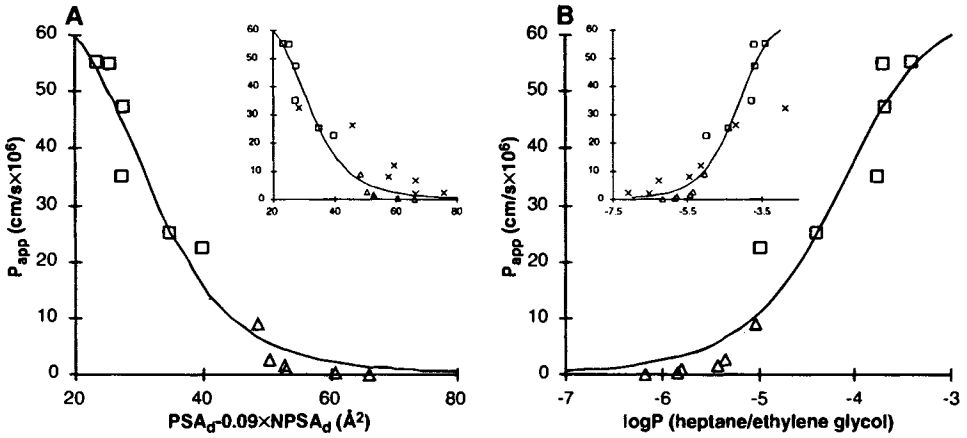

Fig. 4. Sigmoidal relationship between Caco-2 cell monolayer permeability (P_{app}) to and a linear combination of polar and non-polar surface area of two series of dipeptide derivatives, derived as described in the methods section (A). Calculations of the surface properties of the AcHN-X-phenethylamide (□) and AcHN-X-D-Phe-NHMe (Δ) dipeptide derivatives used were based on conformational searches in simulated water. A comparable relationship between heptane-ethylene partitioning of and intestinal permeability to the dipeptide derivatives was obtained (B). The inserts show the corresponding relationships when the model was tested on the D-Phe-oligomers (×), a series of structurally different compounds.

Table II. Correlation Matrix (r) for the Structural and Physico-Chemical Descriptors of the Twelve Dipeptide Derivatives Used for Model Development

	$NPSA_d$[a]	PSA_d[a]	$\%PSA_d$[a]	V_d[a]	$logP_{o/w}$[b]	$logP_{h/w}$[b]	$\Delta logP$[b]	$logP_{h/eg}$[b]
PSA_d[a]	0.254	1						
$\%PSA_d$[a]	−0.441	0.754	1					
V_d[a]	0.984	0.417	−0.279	1				
$logP_{o/w}$[b]	0.681	−0.505	−0.918	0.551	1			
$logP_{h/w}$[b]	0.282	−0.836	−0.954	0.115	0.888	1		
$\Delta logP$[b]	0.261	0.981	0.723	0.425	−0.504	−0.845	1	
$logP_{h/eg}$[b]	0.111	−0.918	−0.923	−0.056	0.778	0.958	−0.894	1
$PSA_d - 0.09 \times NPSA_d$[a]	−0.041	0.956	0.913	0.132	−0.729	−0.949	0.934	−0.982

Note: Molecular surface properties calculated from the geometries of the compounds generated by conformational searches in a simulated water environment are shown.

[a] Determinations of dynamic non-polar surface area ($NPSA_d$), polar surface area (PSA_d) per cent polar surface area ($\%PSA_d$), and volume (V_d) are described in the Methods section.

[b] Data for octanol-water ($logP_{o/w}$), heptane-water ($logP_{h/w}$), and heptane-ethylene glycol ($logP_{h/eg}$) partition coefficients were obtained from (15), as were the difference between the octanol-water and heptane-water partition coefficients ($\Delta logP$).

To our knowledge, this is the first example of a theoretical model that gives a satisfactory relationship between calculated molecular properties and epithelial permeability to peptides by accounting for both the hydrogen bonding capacity and the hydrophobicity.

Molecular descriptors mainly associated with hydrogen bonding, e.g., PSA_d (14) and $\Delta logP$ (23) accounted for the difference in permeability seen between the two series (AcHN-X-phenethylamide and AcHN-X-D-Phe-NHMe derivatives). This is consistent with previous studies, where the polar surface area was shown to be an important descriptor of membrane transport for classes of compounds other than peptides (11,13,14). However, the dipeptide derivatives used for model development in the present paper were designed to display little intraseries variability in hydrogen bonding capacity, as indicated by the small variability in PSA_d and $\Delta logP$ within each series. This is most apparent when considering Ht, which was identical within each respective series (Table I).

Instead, the introduction of non-polar side chains of various sizes resulted in variability in the lipophilicity and size of the molecules within each series. We found that the intraseries variability in P_{app} could be accounted for by molecular descriptors related to size and lipophilicity such as $NPSA_d$ and $logP_{o/w}$ (Fig. 3). Thus, either the hydrogen bonding capacity or lipophilicity/size of compounds, depending on their structure, can predict their transport across cell membranes. We therefore tested the hypothesis that a combination of the descriptors would adequately describe the epithelial permeability to the two series of dipeptide derivatives.

A linear combination of PSA_d and $NPSA_d$ resulted in a strong sigmoidal relationship with P_{app} for the AcHN-X-phenethylamide and AcHN-X-D-Phe-NHMe derivatives (Fig. 4A). The use of conformers generated by conformational searches without solvent did not affect the strength of the relationship between surface properties and P_{app}. However, the relative weight of $NPSA_d$ to PSA_d decreased slightly when the solvent was removed in the conformational analyses. This is not surprising since PSA_d is smaller for conformers generated in vacuum. The decrease in weight of $NPSA_d$ is therefore also an indication of the ability of the dipeptide derivatives to internalize their polar groups when the possibility of interacting with the surrounding water vanishes, i.e. their ability to act as molecular chameleons (24).

$LogP_{h/eg}$, which correlated strongly with $PSA_d - 0.09 \times NPSA_d$, also displayed an excellent sigmoidal relationship with P_{app} (Fig. 4B). Apparently, $logP_{h/eg}$ better describes the relative contributions of hydrogen bonding/polarity and hydrophobicity/solute size to P_{app} than $logP_{o/w}$ and $\Delta logP$. This is in agreement with previous studies, where $logP_{h/eg}$ displayed stronger correlations with intestinal permeability coefficients than $\Delta logP$ and $logP_{o/w}$ (10). An examination of the solvatochromic parameters (25) describing the partition coefficients $logP_{o/w}$, $logP_{h/eg}$ and $\Delta logP$ reveals that the size of the solute is roughly twice as important for octanol-water partitioning than for heptane-ethylene glycol partitioning whereas for $\Delta logP$, the effect of size is negligible (Table III) (23,26).

This is analogous with the molecular surface properties calculated in this study if $NPSA_d$ and $logP_{o/w}$ are considered to be measures of hydrophobicity, which indeed appears to be true within each of the two series of dipeptide derivatives. PSA_d and $\Delta logP$ describe the interactions of the compounds with the surrounding solvent mainly by hydrogen bonding (Table III) (23). In this context, $PSA_d - 0.09 \times NPSA_d$ and $logP_{h/eg}$ describe a situation between these extremes by giving proper weight to both hydrophobic and hydrogen bonding interactions.

How can the strong relationship between P_{app} and $logP_{h/eg}$ observed in the present study be explained? According to studies on the incorporation of lipophilic oligopeptide derivatives into phospholipid membrane vesicles, hydrophobic interactions constitute the major driving force of solute accommodation into the region of polar phospholipid head groups (27 and references therein). In contrast, transfer of these compounds into the interior of the phospholipid bilayer depends mainly on energetically unfavorable interactions between the bilayer and the polar parts of the oligopeptide derivatives (i.e., NH and C=O) and to a lesser extent on hydrophobicity (27).

This is supported by recent advances in molecular dynamics simulations which suggest that solute partitioning into the dense apolar region of the membrane interior is the main barrier in the transport process (28). These results imply that membrane partitioning of oligopeptide derivatives is a two-step process.

Table III. Summary of Solvatochromic Parameters Describing the Partitioning Systems[a]

Equation
$\log P_{o/w} = 5.83(\pm 0.53)V/100 - 0.74\ (\pm 0.31)\pi^* - 3.51\ (\pm 0.38)\beta - 0.15(\pm 0.23)\alpha$ + constant
$\Delta\log P = -0.12(\pm 0.30)\pi^* - 1.96(\pm 0.42)\beta - 3.40(\pm 0.25)\alpha$ + constant
$\log P_{h/w} = 2.79(\pm 0.26)V/100 - 1.53(\pm 0.38)\pi^* - 1.69(\pm 0.29)\beta - 4.41(\pm 0.20)\alpha$ + constant

Note: Values in parenthesis represent the 95% confidence interval of the regression coefficients.

[a] The equations for $\log P_{o/w}$ and $\Delta\log P$ obtained from (23) were derived from regression analysis of 103 and 75 solutes, respectively. The equation for $\log P_{h/w}$ was derived from 20 solutes and obtained from (26). V is the volume, π^* is the dipolarity/polarizability, β is the hydrogen bond acceptor basicity and α is the hydrogen bond donor acidity of the solute. The volume of the solute is roughly twice as important for octanol-water partitioning than for heptane-ethylene glycol partitioning whereas for $\Delta\log P$, the effect of size is negligible.

Lipophilicity is the main determinant for transport of the peptides into the polar head group region of the lipid bilayer and hydrogen bonding/polarity is detrimental for the transport into the non-polar interior of the membrane (3). The latter step may be described by PSA_d or $\Delta\log P$ while the former may be represented by $NPSA_d$ or $\log P_{o/w}$. Thus, depending on which of these two steps is rate determining for the overall membrane permeability, either $PSA_d/\Delta\log P$ or $NPSA_d/\log P_{o/w}$ may be the better descriptor of drug permeation.

In the present study, both of these situations prevail. Thus, the difference in P_{app} values between the two series of dipeptide derivatives is mainly the result of the energetically costly process of transferring an additional amide group from the polar region of the phospholipid head groups to the membrane interior and is therefore best described by PSA_d or $\Delta\log P$. Within each series however, permeation of the molecules across the intestinal membrane is mainly dependent on the hydrophobically driven process of transferring the molecule from the water phase into the polar region of the membrane-water interface and is therefore best described by $NPSA_d/\log P_{o/w}$.

Since $\log P_{h/eg}$ takes both of these effects into account (see above), this descriptor provides a strong relationship with P_{app} for both series of dipeptide derivatives. It has previously been suggested that the good results obtained with $\log P_{h/eg}$ are related to the fact that heptane mimics the non-polar interior of the cell membrane while ethylene glycol mimics the glycerol ester region of the membrane-water interface (26). The results in this study clearly indicate that the heptane-ethylene glycol partitioning system, at least partly, also describes hydrophobic interactions. Given the strong correlation between a combination of surface areas and $\log P_{h/eg}$, we speculate that this is also the case for $PSA_d - 0.09 \times NPSA_d$.

Although the derived model $PSA_d - 0.09 \times NPSA_d$ was tested by a leave-one-out cross-validation procedure it cannot be excluded that the model is less predictive of P_{app} in other data sets, e.g., the series of D-Phe oligomers. In this data set, a systematic underestimation of P_{app} was observed. Despite a thorough analysis of the physico-chemical and calculated molecular descriptors, no explanation for this behavior was found. Nevertheless, the result obtained from this theoretical model is comparable to that of the best experimental descriptor, $\log P_{h/eg}$.

The applicability of the model was also evaluated using an unrelated data set from a previous study (14). In that study, an excellent sigmoidal relationship ($R^2 = 0.94$) was observed between PSA_d of conformers generated by conformational searches without solvent and the absorbed fraction after oral administration to humans for a set of 20 structurally diverse drugs. When PSA_d was substituted for $PSA_d - 0.06 \times NPSA_d$ in that data set R^2 increased to 0.96. This result indicates that a combination of polar and non-polar surface area may be generally applicable for prediction of drug transport. It is important to note that $NPSA_d$ may be strongly correlated to volume (e.g., Table II). Since the diffusion coefficient in the cell membrane decreases steeply as solute size is increased (29), the coefficients in $k_1 \times PSA_d - k_2 \times NPSA_d$ found in this study will be altered if the model is extrapolated to substantially larger compounds. However, by using $NPSA_d$ rather than volume or SA_d as cavity descriptor, this problem will most likely be less pronounced.

Since peptides and peptide derivatives may be substrates for active transporters, the present model was developed using peptide derivatives containing D-amino acids with C-terminal modifications. Transport by the oligopeptide carrier is negligible for such derivatives (30). Further, any influence of efflux by P-glycoprotein was inhibited by verapamil (see methods section, 16). Active transport was avoided since the goal in drug development is to select candidates that do not rely on active transport and avoid efflux systems in order to obtain good oral absorption.

In conclusion, a theoretical model useful for the prediction of epithelial permeability to peptide derivatives has been developed. The method appears also to be promising for other types of compounds and further studies are presently underway to investigate its generality. If this method continues to hold when a larger number of oligopeptides and peptide mimetics have been investigated, it can be used to differentiate poorly absorbed oligopeptides at an early stage of the drug discovery process.

ACKNOWLEDGMENTS

This work was supported by The Swedish Medical Research Council (9478), Centrala försöksdjursnämnden (97-46) and The Swedish Natural Science Research Council (K 11163-301). We would like to acknowledge Dr. J. T. Goodwin, Dr. P. S. Burton and Mr. R. A. Conradi for the design and synthesis of the peptide derivatives reported in this work, along with the partition coefficient and permeability data.

REFERENCES

1. B. Testa and J. Caldwell. Prodrugs revisited: The "Ad Hoc" approach as a complement to ligand design. *Med. Res. Rev.* **16**:233–241 (1996).
2. C. A. Lipinski, F. Lombardo, B. W. Dominy, and P. J. Feeney. Experimental and computational approaches to estimate solubility and permeability in drug discovery and development settings. *Adv. Drug Del. Rev.* **23**:3–25 (1997).

3. P. S. Burton, R. A. Conradi, and A. R. Hilgers. Transcellular mechanisms of peptide and protein absorption: passive aspects. *Adv. Drug Del. Rev.* **7**:365–386 (1991).
4. P. Artursson, K. Palm, and K. Luthman. Caco-2 monolayers in experimental and theoretical predictions of drug transport. *Adv. Drug Del. Rev.* **22**:67–84 (1996).
5. P. Artursson and J. Karlsson. Correlation between oral drug absorption in humans and apparent drug permeability coefficients in human intestinal epithelial (Caco-2) cells. *Biochem. Biophys. Res. Commun.* **175**:880–885 (1991).
6. P. Artursson, J. Karlsson, G. Ocklind, and N. Schipper. In A. J. Shaw (eds), *Cell Culture Models of Epithelial Tissues - a Practical Approach*, Oxford University Press, New York, 1996, pp. 111–133.
7. A. M. ter Laak, R. S. Tsai, G. M. Donné-Op den Kelder, P.-A. Carrupt, B. Testa, and H. Timmerman. Lipophilicity and hydrogen-bonding capacity of H_1-antihistaminic agents in relation to their central sedative side-effects. *Eur. J. Pharm. Sci.* **2**:373–384 (1994).
8. Y. C. Martin. A practioner's perspective of the role of quantitative structure-acitivity analysis in medicinal chemistry. *J. Med. Chem.* **24**:229–237 (1981).
9. P. S. Burton, R. A. Conradi, A. R. Hilgers, N. N. F. Ho, and L. L. Maggiora. The relationship between peptide structure and transport across epithelial cell monolayers. *J. Contr. Rel.* **19**:87–98 (1992).
10. D.-C. Kim, P. S. Burton, and R. T. Borchardt. A correlation between the permeability characteristics of a series of peptides using an *in vitro* cell culture model (Caco-2) and those using an *in situ* perfused rat ileum model of the intestinal mucosa. *Pharm. Res.* **10**:1710–1714 (1993).
11. U. Norinder, T. Österberg, and P. Artursson. Theoretical calulation and prediction of Caco-2 cell permeability using MolSurf parametrization and PLS statistics. *Pharm. Res.* **14**:1785–1790 (1997).
12. H. van de Waterbeemd, G. Camenisch, G. Folkers, and O. A. Raevsky. Estimation of Caco-2 cell permeability using calculated molecular descriptors. *Quant. Struct.-Act. Relat.* **15**:480–490 (1996).
13. K. Palm, K. Luthman, A.-L. Ungell, G. Strandlund, and P. Artursson. Correlation of drug absorption with molecular surface properties. *J. Pharm. Sci.* **85**:32–39 (1996).
14. K. Palm, P. Stenberg, K. Luthman, and P. Artursson. Polar molecular surface properties predict the intestinal absorption of drugs in humans. *Pharm. Res.* **14**:568–571 (1997).
15. J. T. Goodwin, P. S. Burton, A. R. Hilgers, R. A. Conradi, and N. N. F. Ho. Relationships between physicochemical properties for a series of peptides and membrane permeability in Caco-2 cells. *Pharm. Res.* **13**:S243 (1996).
16. P. S. Burton, R. A. Conradi, A. R. Hilgers, and N. N. F. Ho. Evidence for a polarized efflux system for peptides in the apical membrane of Caco-2 cells. *Biochem. Biophys. Res. Commun.* **190**:760–766 (1993).
17. P. Seiler. Interconversion of lipophilicities from hydrocarbon/water systems into octanol/water system. *Eur. J. Med. Chem.* **9**:473–479 (1974).
18. G. Chang, W. C. Guida, and W. C. Still. An internal coordinate Monte Carlo method for searching conformational space. *J. Am. Chem. Soc.* **111**:4379–4386 (1989).
19. F. Mohamadi, N. G. J. Richards, W. C. Guida, R. Liskamp, M. Lipton, C. Caufield, G. Chang, T. Hendrickson, and W. C. Still. MacroModel—An integrated software system for modeling organic and bioorganic molecules using molecular mechanics. *J. Comp. Chem.* **11**:440–467 (1990).
20. J. J. Gajewski, K. E. Gilbert, and J. McKelvey. MMX an enhanced version of MM2. *Adv. Mol. Model.* **2**:65–92 (1990).
21. K. B. Lipkowitz, B. Baker, and R. Larter. Dynamic molecular surface areas. *J. Am. Chem. Soc.* **111**:7750–7753 (1989).
22. J. Karlsson and P. Artursson. A method for the determination of cellular permeability coefficients and aqueous boundary layer thickness in monolayers of intestinal epithelial (Caco-2) cells grown in permeable filter chambers. *Int. J. Pharm.* **71**:55–64 (1991).
23. N. El Tayar, R.-S. Tsai, B. Testa, P.-A. Carrupt, and A. Leo. Partitioning of solutes in different solvent systems: The contribution of hydrogen-bonding capacity and polarity. *J. Pharm. Sci.* **80**:590–598 (1991).
24. B. Testa, P.-A. Carrupt, P. Gaillard, F. Billois, and P. Weber. Lipophilicty in molecular modeling. *Pharm. Res.* **13**:335–343 (1996).
25. M. J. Kamlet, J.-L. M. Abboud, M. H. Abraham, and R. W. Taft. Linear solvation energy relationships. 23. A comprehensive collection of the solvatochromic parameters, π^*,α, and β, and some methods for simplifying the generalized solvatochromic equation. *J. Org. Chem.* **48**:2877–2887 (1983).
26. A. D. Paterson, R. A. Conradi, A. R. Hilgers, V. T. J, and B. P. S. A non-aqueous partitioning system for predicting the oral absorption of peptides. *Quant. Struct.-Act. Relat.* **13**:4–10 (1994).
27. R. E. Jacobs and S. E. White. The nature of the hydrophobic binding of small peptides at the bilayer interfaces: implications for the insertion of transbilayer helices. *Biochemistry.* **28**:3421–3437 (1989).
28. D. P. Tieleman, S. J. Marrink, and H. J. C. Berendsen. A computer perspective of membranes: molecular dynamics studies of lipid bilayer systems. *Biochim. Biophys. Acta.* **1331**:235–270 (1997).
29. T.-X. Xiang and B. D. Anderson. The relationship between permeant size and permeability in lipid bilayer membranes. *J. Membr. Biol.* **140**:111–122 (1994).
30. J. P. F. Bai and G. L. Amidon. Structural specificity of mucosal-cell transport and metabolism of peptide drugs: implication for oral peptide drug delivery. *Pharm. Res.* **9**:969–978 (1992).